HHS Public Access

Author manuscript

J Am Soc Mass Spectrom. Author manuscript; available in PMC 2015 September 01.

Published in final edited form as:

J Am Soc Mass Spectrom. 2014 September ; 25(9): 1592–1599. doi:10.1007/s13361-014-0941-9.

Optimization of Peptide Separations by Differential Ion Mobility Spectrometry

Samantha L. Isenberg, **Paul M. Armistead**, and **Gary L. Glish**

Department of Chemistry, Caudill and Kenan Laboratories, The University of North Carolina at Chapel Hill, Chapel Hill, NC 27599-3290, USA

Abstract

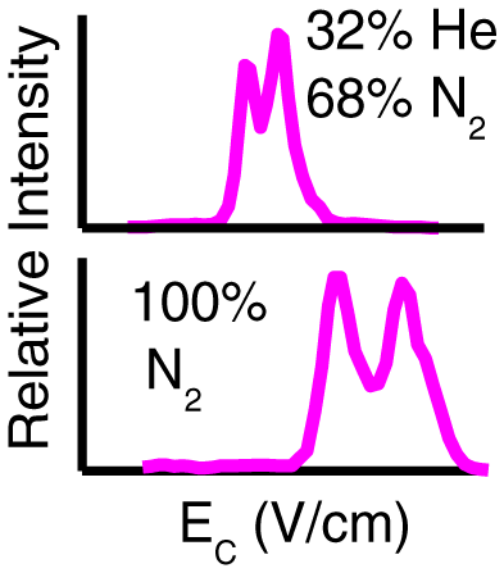

Differential ion mobility spectrometry (DIMS) has the ability to separate gas phase ions based on their difference in ion mobility in low and high electric fields. DIMS can be used to separate mixtures of isobaric and isomeric species indistinguishable by mass spectrometry (MS). DIMS can also be used as a filter to improve the signal-to-background of analytes in complex samples. The resolving power of DIMS separations can be improved several ways, including increasing the dispersion field and increasing the amount of helium in the nitrogen carrier gas. It has been previously demonstrated that the addition of helium to the DIMS carrier gas provides improves separations when the dispersion field is the kept constant as helium content is varied. However, helium has a lower breakdown voltage than nitrogen. Therefore, as the percent helium content in the nitrogen carrier gas is increased, the highest dispersion field accessible decreases. This work presents the trade-offs between increasing dispersion fields and using helium in the carrier gas by comparing the separation of a mixture of isobaric peptides. The maximum resolution for a separation of a mixture of three peptides with the same nominal molar mass was achieved by using a high dispersion field (~72 kV/cm) with pure nitrogen as the carrier gas within the DIMS

Correspondence to: Gary Glish; glish@unc.edu.

assembly. The conditions used to achieve the maximum resolution also exhibit the lowest ion transmission through the assembly, suggesting that it is necessary to consider the trade-off between sensitivity and resolution when optimizing DIMS conditions for a given application.

Keywords

Ion mobility

Introduction

Mass spectrometry is a common detection method used in a wide variety of applications because it provides high sensitivity and resolution with fast analysis times. However, issues such as low signal-to-background, isobaric interferences, and ion suppression can arise with complex samples. To alleviate these drawbacks, separations are frequently used in conjunction with mass spectrometry. Pre-ionization separation techniques such as chromatography and electrophoresis are regularly employed to improve mass spectrometric analyses. Additionally, post-ionization techniques such as ion mobility spectrometry (IMS) can provide a supplementary degree of separation. Because ion mobility is performed post-ionization, these separations will not lessen sensitivity issues due to ionization suppression, but ion mobility techniques hold potential for signal-to-background improvement as well as the elimination of isobaric interferences in complex samples [1–3].

IMS utilizes an applied electric field to separate ions traversing through a buffer gas. Size, shape, charge state, and ion-molecule interactions with the buffer gas govern the mobility of an ion traveling through a collision gas under a given electric field. The velocity of an ion is directly proportional to the reduced electric field, *E/N*, where *E* is the electric field and *N* is the gas number density. At low *E/N*, ion mobility is independent of *E/N*, but as *E/N* is increased, ion mobility becomes dependent on the reduced electric field [4–7]. Differential ion mobility spectrometry (DIMS) utilizes this mobility dependence on electric field to separate ions.

A differential ion mobility spectrometer is comprised of two parallel electrodes with a constant gap between them, to which an rf voltage, alternating between high and low electric fields of opposite polarities, is applied. There are currently two basic DIMS electrode geometries: cylindrical and planar. Cylindrical designs utilize curved electrodes with one electrode having a smaller radius than the other such that the electrodes are parallel throughout the assembly. Cylindrical designs have some advantages over planar DIMS assemblies, including observed increases in ion transmission as the dispersion field is increased due to improved ion focusing [8] and the ability to trap ions at atmospheric pressure [9]. However, the ion focusing effect observed for cylindrical assemblies causes the cylindrical geometry to have lower resolving powers than those observed with planar assemblies [10]. Planar assemblies are also easier to fabricate and have fewer parameters that need to be optimized for a given analysis compared with the cylindrical assemblies. Perhaps most importantly, planar DIMS assemblies can operate in a “transparent mode”

where both electrodes are at ground potential, thus allowing a regular mass spectrum to be obtained without removing the assembly as would be required for cylindrical DIMS.

Whether DIMS is in an active or transparent mode, ions are carried through the gap between the two electrodes by gas flow into the inlet of the mass spectrometer. An asymmetric rf waveform is applied to the electrodes, alternating between low (E_l) and high (E_h) electric fields. During the low-field portion of the waveform (t_l), ions are displaced toward one electrode, a distance proportional to the low field mobility (K_l) of the ion. During the high field portion of the waveform (t_h), ions are displaced toward the other electrode, a distance proportional to the high field mobility (K_h) of the ion (Equations 1 and 2) [6].

$$d_l = K_l E_l t_l \quad (1)$$

$$d_h = K_h E_h t_h \quad (2)$$

During the transit time through the DIMS assembly, ions are separated by their net displacement (d_h-d_l) towards one of the electrodes. The waveform is applied such that $E_l t_l = E_h t_h$ and thus the net displacement of an ion is directly proportional to the difference between high and low field mobilities (K_h-K_l). The $V_{0\text{-}P}$ of the waveform is commonly referred to as the dispersion voltage, *DV*, or expressed in terms of electric field (E_D) by dividing the DV by the distance between the electrodes or the gap (g). The dispersion field is equivalent to E_h in the above equations. Assuming $E_l t_l = E_h t_h$, an ion with $K_h \neq K_l$ would have no net displacement, whereas ions with K_h K_l would be neutralized on the electrodes. A DC offset, or compensation voltage (*CV*), can be applied to one of the electrodes to counterbalance the displacement of the ion, allowing only ions with the selected K_h-K_l to pass through the assembly. The *CV* is often expressed as a compensation field (E_C) by dividing the *CV* by the gap between the electrodes. The E_C can be held constant during an experiment, using DIMS in filter mode to select for a beam of ions with a given K_h-K_l. Alternatively, DIMS can be used in scanning mode for a specified *CV* range.

In the low field, ions with smaller collisional cross-sections will undergo fewer collisions with the counter-current gas and have higher mobilities than ions with larger collisional cross-sections. High field mobility is not as well understood as low field mobility; the direct proportionality between ion mobility and collisional cross-section no longer holds true. This means that DIMS is more orthogonal to MS than conventional IMS, but also that it is not currently possible to predict the E_C of an ion under a given set of conditions, even if the collisional cross-section is known. Additionally, it is unclear what conditions will provide the best resolution and sensitivity for a given sample.

The resolving power of DIMS can be improved by increasing the applied dispersion field (E_D), or by increasing the separation time [11]. Some analytes exhibit an improvement in resolving power as the carrier gas composition (commonly 100% nitrogen) is changed by introducing helium or other gases. Resolving power can also be improved by adding organic dopants to the carrier gas, which alters ion mobility [12–18]. Although helium improves the separation power of DIMS at a given E_D, there are several drawbacks to the use of helium in

the carrier gas. Helium has a lower pumping efficiency than nitrogen, so the use of helium in the carrier gas causes elevated pressures in the fore region of the mass spectrometer and can lead to failure of the pumping system. Additionally, adding helium in DIMS lowers the breakdown voltage in the gap between the electrodes [19] and, thus, higher dispersion fields are accessible with pure nitrogen as the carrier gas than with helium added. Thus, in optimizing the resolving power of DIMS, there is a trade-off between the highest dispersion field accessible and the percentage of helium in the carrier gas: as the helium content is increased, the maximum E_D is decreased. Previous work with helium in the DIMS carrier gas compares the separation power with the same E_D, but does not address the change in the maximum electric field accessible with helium. Owing to the trade-off between these two parameters, a comparison of DIMS performance needs to be made using the maximum E_D achievable for different percentages of helium in the nitrogen carrier gas. This work compares the performance of DIMS under various carrier gas conditions to optimize the separation of a mixture of isobaric peptides.

Experimental

Peptides (Table 1) were purchased and used without further purification (New England Peptide, Gardner, MA, USA). Methanol (HPLC grade), water (HPLC grade), and acetic acid (ACS plus) were purchased from Fisher Scientific, Fairlawn, NJ, USA. Peptide solutions (5–20 μM) for electrospray ionization (ESI) were prepared in 49.5/49.5/1 (v/v/v) methanol/water/acetic acid and were infused at a flow rate of 2 μL/min. All experiments used a Bruker Esquire 3000 ion trap mass spectrometer. A voltage of 4.25 kV was applied to the electrospray emitter. The temperature of the ESI desolvation gas was set in the software to a value of 300°C, and the flow rate of the desolvation gas was varied from 2.5 to 7.5 L/min. The temperature of the DIMS electrodes increases from 53 to 111ºC as the desolvation gas flow rate is increased from 2.5 to 7.5 L/min at a temperature setting of 300°C. The temperature reading in the software is given by a sensor near the heater, which is oriented near the glass transfer capillary. The temperature at the inlet of the DIMS assembly changes with the flow rate of the desolvation gas because the gas must travel around the transfer capillary and through the DIMS assembly.

A planar DIMS assembly (Figure 1) was used for these experiments. The two parallel stainless steel 6 × 25 mm electrodes are separated by a 0.3 mm gap. The DIMS assembly is threaded to match the Apollo I spray shield of a Bruker Esquire 3000, such that the spray shield can be removed, and the DIMS assembly can be screwed on in its place. In this design, the desolvation gas, which is already implemented in the Apollo I source for desolvation purposes, is redirected through the housing of the assembly, utilizing the desolvation gas as the carrier gas through the DIMS assembly as well as for desolvation when coupled to electrospray ionization (ESI). The ratio of helium to nitrogen in the carrier gas was varied using two MKS model 1179 mass flow controllers regulated by a LabVIEW program and routed into the desolvation gas line. The standard glass transfer capillary of the source was replaced with a custom flared glass transfer capillary [20].

A custom-built power supply (Ridgeway and Glish, In prep.) was used for these experiments. Ideally, a square wave should be used for DIMS, alternating between low and

high electric fields of opposing polarity. However, because of the high power requirements of high voltage, high frequency square waves, most DIMS waveforms are bisinusoidal, approximating a square wave [6]. In this design, one sinusoidal voltage at a given frequency and amplitude is applied to one of the electrodes, a phase-shifted sinusoidal voltage at twice the frequency, and approximately one-half the amplitude is applied to the other electrode, and the voltages are capacitively summed across the gap between the electrodes (Figure 2). The dispersion voltage (*DV*) is defined by the maximum voltage of the bisinusoidal waveform. The dispersion field (E_D) is defined as the *DV* divided by the distance between the DIMS electrodes, or the gap (*g*). The bisinusoidal DIMS waveform was tuned with a sine wave at 1.7 MHz on one electrode and a sine wave at 3.4 MHz on the other electrode. DIMS scans were carried out using a LabVIEW program linked to the instrument control software. A static compensation voltage for filter mode can also be selected with the LabVIEW program.

A DIMS scan can be plotted by tracing the total ion current or the extracted ion current as a function of the E_C. The resolving power (*RP*) of a given peak is often used to evaluate DIMS performance (Equation 3). Resolving power values were calculated using a Mathematica script, written to approximate the FWHM of a peak, assuming Gaussian distributions. Additionally, the separation of two peaks in a mixture can be calculated by determining the resolution, (*R*), between the two peaks (Equation 4). Resolutions were calculated using the Fit Multi-peaks analysis function in Microcal Origin 6.0.

$$RP = \frac{CV}{FWHM} \quad (3)$$

$$R = \frac{CV_2 - CV_1}{\left(\frac{w_1 + w_2}{2}\right)} = \frac{1.178(CV_2 - CV_1)}{(FWHM_1 + FWHM_2)} \quad (4)$$

Ion transmission was determined for the DIMS operating parameters by comparing signal intensity with DIMS active to that which is obtained with the assembly removed (Equation 5). The average signal with DIMS was determined by averaging over a 2-min acquisition period the signal observed for the protonated peptide with E_C set for at the value where maximum ion intensity is observed.

$$\%Ion\ Transmission = \frac{signal\ with\ DIMS}{signal\ without\ DIMS} \times 100\% \quad (5)$$

Results and Discussion

Improving Resolution of DIMS separations

An increase in the dispersion field (E_D) of the DIMS waveform increases the resolution of DIMS separations [21, 22], but also leads to a decrease in ion transmission through the assembly. Because the displacement of an ion is directly proportional to the applied electric field (Equations 1 and 2), the oscillation amplitude of the ion (Δd) will increase with

increasing electric field strength, effectively constraining the analytical gap between the electrodes [23]. Thus, the effective analytical gap (g_e) can be described by Equation 6, and Δd is described by Equation 7, where P is one period of the waveform and K is the ion mobility, which changes with the electric field [22]. When the effective gap is larger, more ions are allowed to pass through the device than with a smaller effective gap, reducing the resolution and specificity of DIMS, but increasing the ion transmission through the assembly.

$$g_e = g - \Delta d \quad (6)$$

$$\Delta d = \frac{1}{2}\int_0^P |K E_D(t)| dt \quad (7)$$

Using helium in the carrier gas improves the resolution of DIMS separations [14–17]. With all other parameters held constant, the addition of helium has a similar effect as increasing the E_D, improving the separation of the mixture at the expense of signal intensity. The absolute mobility of an ion increases with an increasing percent of helium in nitrogen because ions have a longer mean free path in helium compared with nitrogen. Therefore, it is expected that the addition of helium will cause an increase in the lateral diffusion of ions, causing a decrease in the ion transmission through the assembly. It is also expected that the addition of helium will increase the amplitude of ion oscillation within the gap (Δd), thereby decreasing the effective analytical gap. This increases the resolving power of DIMS separations, but causes a greater percentage of ions to be neutralized on the electrodes.

While helium improves the separation power of DIMS at a given E_D, there are a few drawbacks to the use of helium in the carrier gas, including a lower pumping efficiency than nitrogen, which causes elevated pressures in the fore region of the mass spectrometer. Many commercial instruments have a failsafe that will automatically shut down the instrument if the pressure rises above a given threshold. Although pumping issues can be alleviated by instrument design, the addition of helium to the carrier gas also causes a decrease in the breakdown voltage in the DIMS gap [19] compared with nitrogen. The breakdown voltage is an inherent property of the instrument and the gas composition. Therefore, higher dispersion fields are accessible with pure nitrogen as the carrier gas than with helium added.

At a given percentage of helium in nitrogen, the highest resolving power achievable will be under conditions with the highest E_D possible. To determine which condition gives the best performance, the DIMS waveform was tuned up to the maximum E_D accessible for 0%, 16%, and 32% helium in nitrogen. The ion transmission was calculated for the peptides YLFTLEPQT (a), LLSLLLLMPV (b), AMNGVIFLV (c), and SVSIYTPVV (d) under each condition. The signal without DIMS was determined using 100% N_2 as the desolvation gas for these calculations. The resolving power was also determined with individual solutions of AMNGVIFLV and SVSIYTPVV to compare the performance of the DIMS assembly under each condition. Finally, the resolution of a mixture of two peptides with the same nominal molar mass, YLFTLEPQT and LLSLLLLMPV, was determined under each condition (Table 2).

The resolving power did not show a clear trend favoring a higher dispersion field or a higher percentage of helium in the carrier gas when using the maximum E_D for each *%He*. A decrease in E_D is expected to reduce the resolving power of DIMS, but because the amount of helium can be increased as the E_D is decreased, the net effect on resolving power is statistically insignificant. Although a calculated resolving power is helpful in describing the performance of the DIMS assembly, it does not provide information about the separation of two peaks. For the separation of YLFTLEPQT and LLSLLLLMPV, the average resolution (n = 3) was maximized with a E_D of 74 kV/cm and 0% helium added to the nitrogen carrier gas. These data also show a trend in ion transmission across the three different conditions. The highest percentage of helium investigated for these peptides did exhibit a reduction in resolution, but still exhibited an increase in ion transmission because the E_D was lowered. At a constant E_D, an increase in the ratio of helium to nitrogen has been shown to decrease the ion transmission [16]. However, when the maximum E_D is used for each ratio an increase in ion transmission is observed with increasing helium content.

With the DIMS design used for these experiments, the desolvation gas flow can be varied to manipulate the temperature of the carrier gas between the electrodes of the DIMS assembly. With a desolvation gas temperature setting of 300ºC, the temperature of the electrodes is 53ºC at a flow rate of 2.5 L/min, 84ºC at 5 L/min, and 111ºC at 7.5 L/min. With an increase in the temperature, the gas number density (N) in the analytical gap decreases because the pressure is constant. Thus, *E/N* increases with increasing carrier gas temperature causing a shift in the observed E_C of a given ion [24, 25]. The desolvation gas flow rate for the above experiments was 5 L/min. Using the mixture of YLFTLEPQT and LLSLLLLMPV, the resolution was determined at various desolvation gas flow rates, using 100% nitrogen and a fixed E_D of 72 kV/cm (Figure 3). These data confirm that for these isobaric peptides, the resolution increases from 0 to 1.26 as the desolvation gas flow rate increases from 2.5 to 7.5 L/min at a constant E_D. As with the increased electric fields and helium dopants, increasing the temperature within the gap causes a decrease in ion transmission through the DIMS assembly. It should be noted that as the desolvation gas flow rate is lowered, an increase in the presence of solvent vapor in the gap may be contributing to the observed changes in separation [13, 18], although we have not seen shifts in E_C in previous experiments using dopants in the desolvation gas.

In the DIMS assembly used for these experiments, varying the desolvation gas flow rate does not affect the ion residence time in DIMS. The DIMS assembly is coupled to a glass transfer capillary through which ions are drawn into the mass spectrometer. This glass capillary has a conductance limit of approximately 1.4 L/min. Because of this conductance limit, the volumetric gas flow rate through the DIMS assembly, which dictates the residence time of ions, does not change as the desolvation gas flow is varied. If the separation time is increased for a DIMS separation, the resolving power improves, but the centroid E_C of the peak of interest remains the same [12]. Because the centroid E_C of the peak of interest changes when the desolvation gas flow is varied, this indicates that separation time is not the reason for the observed changes in resolving power. Therefore, the increase in resolving power with an increase in the desolvation gas flow rate cannot be explained by a change in separation time, but rather a change in temperature of the gas within the DIMS assembly.

Optimized Separation of Three Isobaric Peptides

Three peptides (YLFTLEPQT, LLSLLLLMPV, and ILSFVFIMAA) that have the same nominal molar mass (1111 g/mol) were used to determine if DIMS would provide the resolution necessary to separate peptides of similar mass and polarity. Owing to their similarity in mass, conventional tandem mass spectrometry techniques cannot isolate one peptide from the others to produce distinct MS/MS spectra when they are ionized as a mixture. The peptides are primarily composed of hydrophobic residues, making them difficult to separate by polarity using chromatographic methods. DIMS separates ions based on K_h-K_l and is complementary to mass spectrometry, so it has potential for the use as a separation method for these peptides.

Using the enhanced resolution with the high dispersion field strength (72 kV/cm) achievable with 100% nitrogen as the carrier gas, the mixture of three peptides was separable, with two of the three peptides baseline-resolved from each other [Figure 4, note that there is an order of magnitude difference in the scale between part (a) and part (d)]. The three peptides were not separable with helium added to the carrier gas. Each peptide can be selected by applying the E_C for its maximum transmission: 460 V/cm for YLFTLEPQT, 397 V/cm for LLSLLLLMPV, and 430 V/cm for ILSFVFIMAA. Collision-induced dissociation was used to produce tandem mass spectra (MS/MS) at each E_C (Figure 5b, c, and d). Additionally, an MS/MS spectrum of the mixture was collected without DIMS to show the convolution of product ions from the three different isobaric parent ions (Figure 5a). Although the three peptides are not all baseline-resolved from each other (Figure 4), minimal overlap is observed in the MS/MS spectra. In the MS/MS spectrum obtained when selecting for ILSFVFIMAA, four product ions are observed that correspond to product ions of LLSLLLLMPV. The high relative intensity of the ions from LLSLLLLMPV is partially due to the low absolute intensity of ILSFVFIMAA compared with the other two peptides. ILSFVFIMAA consistently produced lower ion signal at a given concentration than the other two peptides, both with and without DIMS installed. The concentration of ILSFVFIMAA in this experiment was 10 μM, double that of the other two peptides. Even with the increased concentration, the peak corresponding to ILSFVFIMAA is lower intensity than the other two peptides in the mixture, making the peak unobservable in the DIMS scan of the mixture (Figure 4a). However, the MS/MS spectrum of ILSFVFIMAA can still be obtained from the mixture by applying the E_C corresponding to the maximum transmission of that ion (Figure 5d) even though a distinct peak is not observable in the DIMS scan.

Conclusions

In this study, the fact that the addition of helium to the carrier gas will reduce the maximum dispersion field achievable is taken into account by comparing separations using the greatest field accessible for each carrier gas composition investigated. For the peptides investigated in this study, the resolution and resolving power were maximized with 100% nitrogen as the carrier gas, where a higher electric field is achievable than with helium added to the carrier gas. Ion transmission was maximized by increasing the percent helium in the carrier gas and, in turn, lowering the maximum electric field strength. For a constant electric field, the

addition of helium causes a decrease in ion transmission. However, comparing the data obtained with maximized electric fields for each condition, the ion transmission is greatest when helium is added because a the maximum electric field is lowered with helium as compared to pure nitrogen.

To separate a mixture of three isobaric peptides, pure nitrogen had to be used as the carrier gas to achieve the maximum resolution at a dispersion field that is unattainable with helium added to the carrier gas. For the separation of the three isobaric peptides, the flow rate of the desolvation gas was elevated to increase the temperature in the DIMS assembly. The conditions needed to achieve the best resolution also caused the greatest decrease in ion transmission through the assembly. For DIMS separations, as is common for most analytical techniques, it is necessary to consider the trade-off between sensitivity and resolution when optimizing conditions for a given application.

Acknowledgments

The authors thank Melvin Park, Desmond Kaplan, Mark Ridgeway, and Joel Kandel from Bruker Daltonics for their continued support with the development of the planar DIMS assembly. Bruker has licensed some of the DIMS technology developed in the Glish lab.

References

1. Kolakowski BM, Mester Z. Review of applications of high-field asymetric waveform ion mobility spectrometry (FAIMS) and differential ion mobility spectrometry (DMS). Analyst. 2007; 132:842–864. [PubMed: 17710259]
2. Xia Y, Wu ST, Jemal M. LC-FAIMS-MS/MS for quantification of a peptide in plasma and evaluation of FAIMS global selectivity from plasma components. Anal Chem. 2008; 80:7137–7143. [PubMed: 18652493]
3. Hatsis P, Valaskovic G, Wu J. Online nanoelectrospray/high-field asymmetric waveform ion mobility spectrometry as a potential tool for discovery pharmaceutical bioanalysis. Rapid Commun Mass Spectrom. 2009; 23:3736–3742. [PubMed: 19902415]
4. Eiceman, G.; Karpas, Z. Ion Mobility Spectrometry. CRC Press; Boca Raton: 2005.
5. Mason, EA.; McDaniel, EW. Transport Properties of Ions in Gases. John Wiley & Sons Inc; New York: 1988.
6. Purves RW, Guevremont R, Day S, Pipich CW, Matyjaszcyk MS. Mass spectrometric characterization of a high-field asymmetric waveform ion mobility spectrometer. Rev Sci Instrum. 1998; 69:4094–4105.
7. Shvartsburg, AA. Differential Ion Mobility Spectrometry. CRC Press; Boca Raton: 2009.
8. Guevremont R, Purves RW. Atmospheric pressure ion focusing in a high-field asymmetric waveform ion mobility spectrometer. Rev Sci Instrum. 1999; 70:1370–1383.
9. Guevremont R, Ding LY, Ellis B, Barnett DA, Purves RW. Atmospheric pressure ion trapping in a tandem FAIMS-FAIMS coupled to a TOFMS: studies with electrospray generated gramicidin S ions. J Am Soc Mass Spectrom. 2001; 12:1320–1330. [PubMed: 11766759]
10. Shvartsburg AA, Li FM, Tang KQ, Smith RD. High-resolution field asymmetric waveform ion mobility spectrometry using new planar geometry analyzers. Anal Chem. 2006; 78:3706–3714. [PubMed: 16737227]
11. Shvartsburg AA, Smith RD. Ultrahigh-resolution differential ion mobility spectrometry using extended separation times. Anal Chem. 2011; 83:23–29. [PubMed: 21117630]
12. Shvartsburg AA, Tang KQ, Smith RD. Understanding and designing field asymmetric waveform ion mobility spectrometry separations in gas mixtures. Anal Chem. 2004; 76:7366–7374. [PubMed: 15595881]

13. Schneider BB, Covey TR, Coy SL, Krylov EV, Nazarov EG. Chemical effects in the separation process of a differential mobility/mass spectrometer system. Anal Chem. 2010; 82:1867–1880. [PubMed: 20121077]
14. Cui M, Ding L, Mester Z. Separation of cisplatin and its hydrolysis products using electrospray ionization high-field asymmetric waveform ion mobility spectrometry coupled with ion trap mass spectrometry. Anal Chem. 2003; 75:5847–5853. [PubMed: 14588025]
15. Shvartsburg AA, Tang KQ, Smith RD. Differential ion mobility separations with resolving power exceeding 50. Anal Chem. 2010; 82:32–35. [PubMed: 19938817]
16. Shvartsburg AA, Danielson WF, Smith RD. High-resolution differential ion mobility separations using helium-rich gases. Anal Chem. 2010; 82:2456–2462. [PubMed: 20151640]
17. Shvartsburg AA, Creese AJ, Smith RD, Cooper HJ. Separation of a set of peptide sequence isomers using differential ion mobility spectrometry. Anal Chem. 2011; 83:6918–6923. [PubMed: 21863819]
18. Rorrer LC, Yost RA. Solvent vapor effects on planar high-field asymmetric waveform ion mobility spectrometry. Int J Mass Spectrom. 2011; 300:173–181.
19. Paschen F. Ueber die zum Funkenübergang in Luft, Wasserstoff, und Kohlensäure bei verschiedenen Drucken erforderliche Potentialdifferenz. Ann Phys. 1889; 273:69–96.
20. Bushey JM, Kaplan DA, Danell RM, Glish GL. Pulsed nano-electrospray ionization: characterization of temporal response and implementation with a flared inlet capillary. Instrum Sci Technol. 2009; 37:257–273. [PubMed: 21785563]
21. Purves RW, Guevremont R. Electrospray ionization high-field asymmetric waveform ion mobility spectrometry mass spectrometry. Anal Chem. 1999; 71:2346–2357. [PubMed: 21662783]
22. Shvartsburg AA, Prior DC, Tang K, Smith RD. High-resolution differential ion mobility separations using planar analyzers at elevated dispersion fields. Anal Chem. 2010; 82:7649–7655. [PubMed: 20666414]
23. Buryakov IA. Mathematical analysis of ion motion in a gas subjected to an alternating-sign periodic asymmetric-waveform electric field. Tech Phys. 2006; 51:16–21.
24. Krylov EV, Coy SL, Nazarov EG. Temperature effects in differential mobility spectrometry. Int J Mass Spectrom. 2009; 279:119–125.
25. Barnett DA, Belford M, Dunyach J, Purves RW. Characterization of a temperature-controlled FAIMS system. J Am Soc Mass Spectrom. 2007; 18:1653–1663. [PubMed: 17662612]

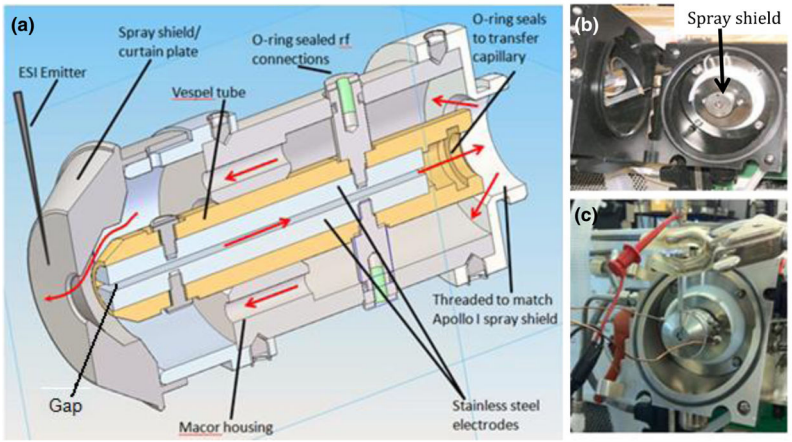

Figure 1.

(a) Planar DIMS assembly with major parts labeled. Gas flow is indicated by red arrows. **(b)** Apollo I source with spray shield attached. **(c)** Apollo I source with spray shield removed and DIMS attached

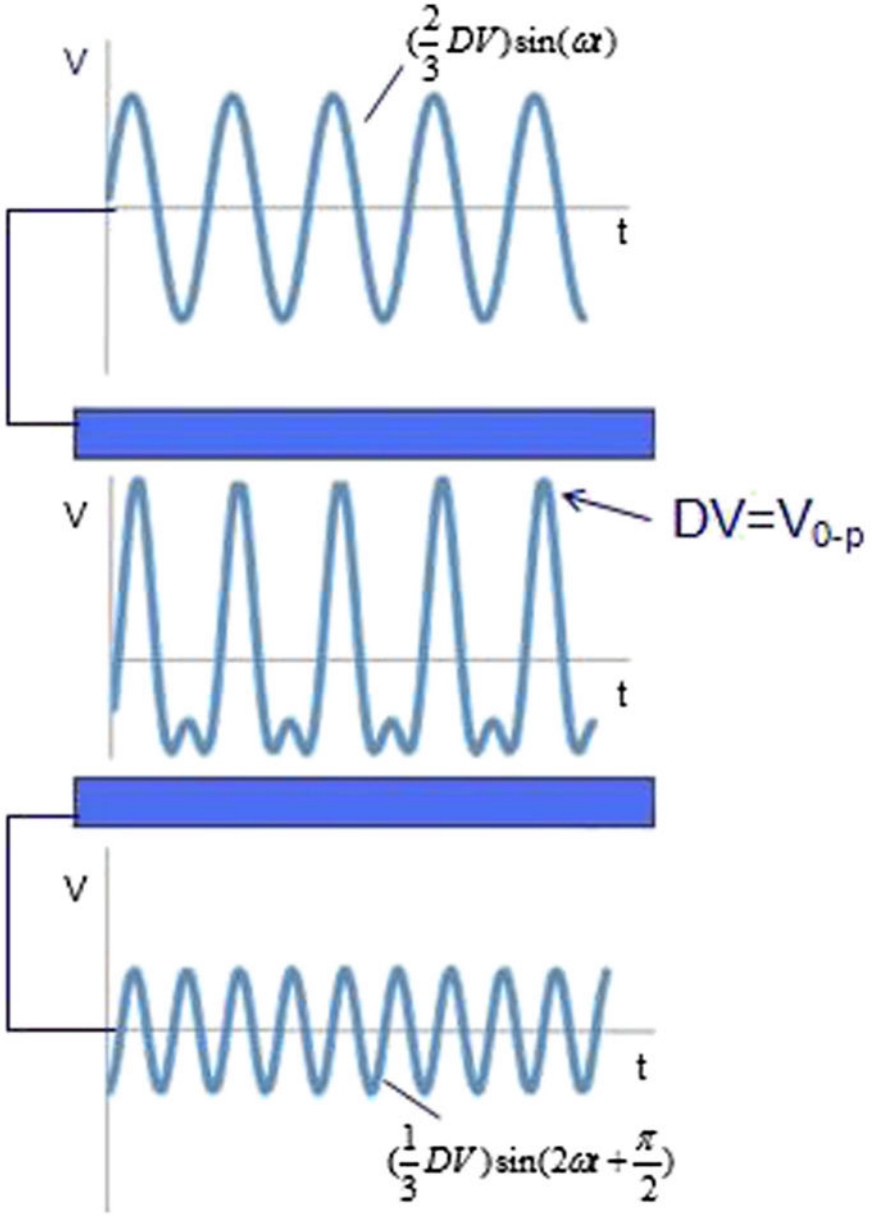

Figure 2.
Simplified schematic of the addition of two sinusoidal waves across the gap to create the bisinusoidal waveform

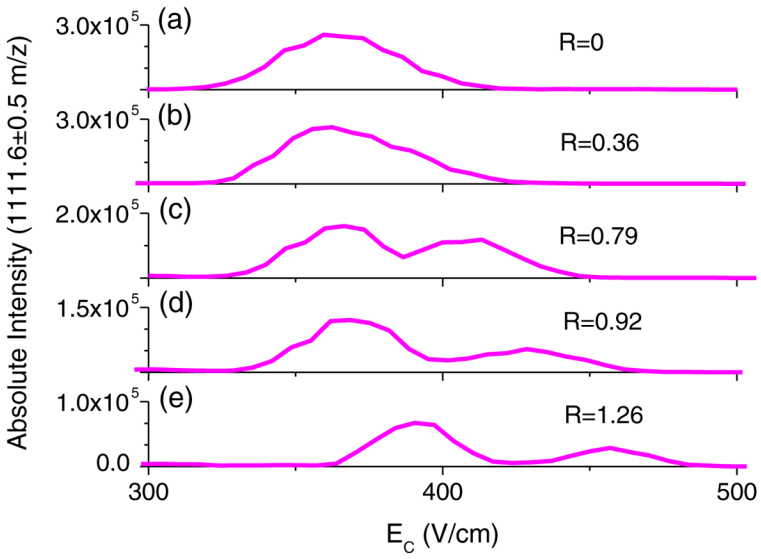

Figure 3.

DIMS scans obtained as desolvation gas flow rate is varied at a fixed E_D of 72 kV/cm; **(a)** 2.5 L/min, **(b)** 4 L/min, **(c)** 5 L/min, **(d)** 6 L/min, and **(e)** 7.5 L/min. Resolution was calculated at each flow rate

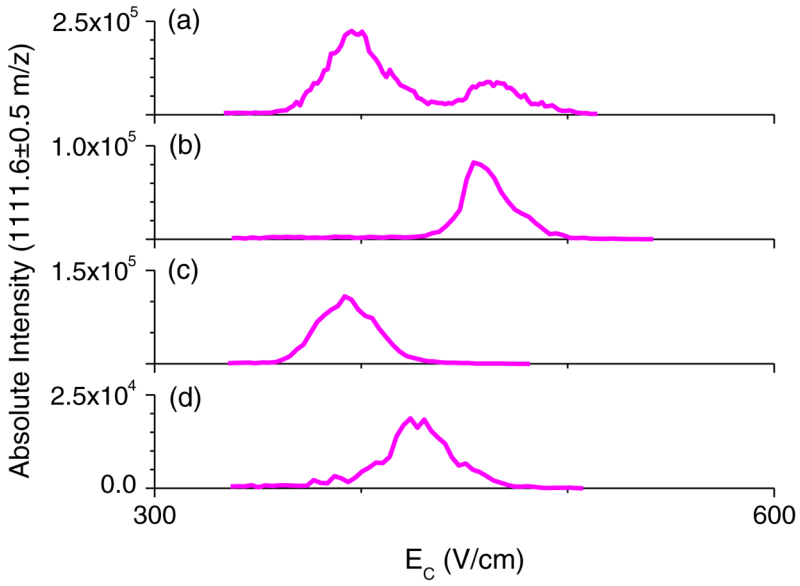

Figure 4.

DIMS scans of isobaric peptides. **(a)** Mixture of 5 μM YLFTLEPQT, 5 μM LLSLLLLMPV, and 10 μM ILSFVFIMAA; **(b)** pure 5 μM YLFTLEPQT, **(c)** pure 5 μM LLSLLLLMPV, and **(d)** Pure 10 μM ILSFVFIMAA

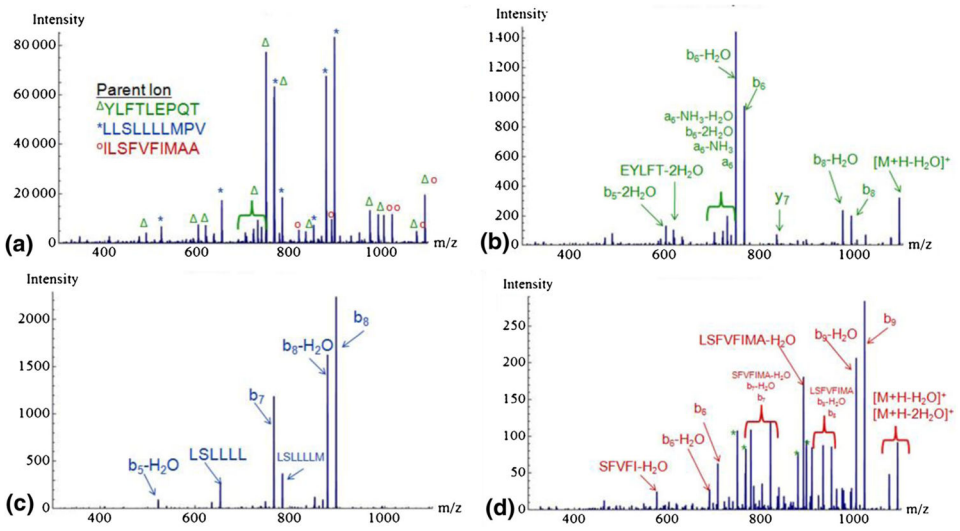

Figure 5.

MS/MS spectra of a mixture of nominally isobaric peptides. **(a)** MS/MS of peptide mixture without DIMS; **(b)** MS/MS of mixture at fixed E_C of 460 V/cm, selecting for LLSLLLLMPV; **(c)** MS/MS of mixture at fixed E_C of 397 V/cm, selecting for YLFTLEPQT; **(d)** MS/MS of mixture at fixed E_C of 430 V/cm, selecting for ILSFVFIMAA. Green stars correspond to residual product ions from YLFTLEPQT, which can be reduced by applying a slightly higher E_C

Table 1

List of Peptides

Peptide Sequence	*m/z* of $[M+H]^+$
YLFTLEPQT	1111.5670
LLSLLLLMPV	1111.7159
ILSFVFIMAA	1111.6220
AMNGVIFLV	963.5332
SVSIYTPVV	964.5350

Table 2

Ion Transmission, Resolving Power, and Resolution for Each % Helium (n = 3). Peptides are Designated as Follows: (a) YLFTLEPQT, (b) LLSLLLLMPV, (c) AMNGVIFLV, and (d) SVSIYTPVV

% He	Maximum E_D (kV/cm)	%T				RP		R (a&b)
		a	b	c	d	c	d	
0	74	0.93 ± 0.13	1.70 ± 0.21	0.87 ± 0.11	0.75 ± 0.12	14. 01 ± 0.57	12.52 ± 0.97	0.73 ± 0.12
16	68	1.85 ± 0.20	5.66 ± 0.61	1.81 ± 0.21	0.84 ± 0.26	14.19 ± 1.12	12.83 ± 3.33	0.63 ± 0.12
32	57	2.04 ± 0.24	7.63 ± 0.76	5.31 ± 0.46	1.43 ± 0.27	12.01 ± 1.51	9.27 ± 1.23	0.50 ± 0.08